Reversible Monoclinic–Rhombohedral Transformation in $LiSn_2(PO_4)_3$ with NASICON-Type Structure

Ana Martínez-Juárez, José M. Rojo,* Juan E. Iglesias, and Jesús Sanz

Instituto Ciencia de Materiales de Madrid, CSIC, Serrano 115 dpdo, 28006 Madrid, Spain

Received March 3, 1995. Revised Manuscript Received June 16, 1995[⊗]

A reversible monoclinic–rhombohedral transformation has been found in $LiSn_2(PO_4)_3$ with NASICON-type structure. The transformation has been followed by XRD, NMR (^{119}Sn, ^{31}P, and ^{7}Li), and DSC techniques, while the sample is heated and cooled in the range 10–250 °C. The monoclinic-to-rhombohedral transformation progresses at temperatures above 100 °C, the transformation goes back between 60 and 10 °C, and it defines a hysteresis cycle in temperature. The enthalpy involved in the transition is 8 kJ/mol, and the cell volume becomes greater by 1.17% in the rhombohedral phase. The electrical conductivity due to diffusion of Li^+ ions has been estimated as a function of sample temperature from impedance measurements. The conductivity values are higher in the monoclinic phase, and the activation energy is 0.49 and 0.71 eV for the monoclinic and rhombohedral phases, respectively. A change in conductivity during the phase transition has been observed.

Introduction

In materials of composition $LiM_2(PO_4)_3$, M^{IV} = Ge, Ti, Sn, Zr, etc., with NASICON-type structure the framework is built up by $M_2(PO_4)_3$ units, which consist of two MO_6 octahedra linked to each other by three PO_4 tetrahedra.[1-3] The Li^+ ions can be placed in two different sites: one, in a distorted octahedral oxygen environment at the intersection of three conduction channels (M1 site) and the other, at each bend of the conduction channel in a polyhedron of eight neighboring oxygens (M2 site).

For the compositions in which the crystal structure has been solved a rhombohedral $R\bar{3}c$ symmetry has been found.[1-10] However, in several cases, a lower symmetry has been reported.[1,11-13] In fact, samples of $LiSn_2(PO_4)_3$ with different symmetry have been prepared from a stoichiometric mixture of Li_2CO_3, SnO_2, and $(NH_4)_2HPO_4$ calcined at different temperatures. A powder sample was first obtained at 950 °C, and its X-ray diffractogram was indexed by using a rhombohedral $R\bar{3}c$ cell.[14] Later, two phases were prepared:[15] one by calcination at 950 °C, and the other at 1250 °C. Their X-ray diffraction patterns were indexed on the basis of two different rhombohedral $R\bar{3}c$ cells, although some of the peaks observed in the pattern of the sample prepared at 950 °C could not be indexed. Recently, the formation process of $LiSn_2(PO_4)_3$ from the already mentioned stoichiometric mixture has been studied[16] by XRD, NMR (^{119}Sn, ^{31}P, and ^{7}Li), and TG techniques. By calcination the stoichiometric mixture at 1200 °C a pure phase of $LiSn_2(PO_4)_3$, called phase I, was obtained. The NMR and XRD data supported a monoclinic *Cc* symmetry. Another phase of $LiSn_2(PO_4)_3$, called phase II, was obtained by calcination the stoichiometric mixture in the range 450–1100 °C. However, this phase always coexisted with other products such as phase I, SnO_2 and SnP_2O_7, the last one being an intermediate compound easily formed.[16,17] The X-ray diffraction pattern of phase II could not be indexed, and the spectroscopic data agreed with a rhombohedral $R\bar{3}c$ symmetry.[16]

On the other hand, it is known that the NASICON structure can change with temperature, and some phase transformations have been detected. For instance, $LiZr_2(PO_4)_3$ shows two phase transitions:[1,12] one about 40 °C in which the symmetry changes from monoclinic to rhombohedral, and the other about 300 °C in which the rhombohedral structure is transformed into another rhombohedral one. Furthermore, phase transitions of the NASICON-type materials, which are in general good conductors of alkali ions,[4,18-39] affect notably the electri-

[⊗] Abstract published in *Advance ACS Abstracts,* August 15, 1995.

(1) Petit, D.; Colomban, Ph.; Collin, G.; Boilot, J. P. *Mater. Res. Bull.* **1986**, *21*, 365.
(2) Tran Qui, D.; Hamdoune, S.; Soubeyroux, J. L.; Prince, E. *J. Solid State Chem.* **1988**, *72*, 309.
(3) Alami, M.; Brochu, R.; Soubeyroux, J. L.; Gravereau, P.; Le Flem, G.; Hagenmuller, P. *J. Solid State Chem.* **1991**, *90*, 185.
(4) Goodenough, J. B.; Hong, H. Y.-P.; Kafalas, J. A. *Mater. Res. Bull.* **1976**, *11*, 203.
(5) Hong, H. Y.-P. *Mater. Res. Bull.* **1976**, *11*, 173.
(6) Hagman, L.; Kierkegaard, P. *Acta Chem. Scand.* **1968**, *22*, 1822.
(7) Sljukic, M.; Matkovic, B.; Prodic, B.; Anderson, D. *Z. Kristallogr.* **1969**, *130*, 148.
(8) McCarron, E. M.; Calabrese, J. C.; Subramanian, M. A. *Mater. Res. Bull.* **1987**, *22*, 1421.
(9) Mbandza, A.; Bordes, E.; Courtine, P.; El Jazouli, A.; Le Flem, G.; Hagenmuller, P. *React. Solids* **1988**, *5*, 315.
(10) Leclaire, A.; Borel, M. M.; Grandin, A.; Raveau, B. *Mater. Res. Bull.* **1991**, *26*, 207.
(11) Casciola, M.; Costantino, U.; Merlini, L.; Krogh Andersen, I. G.; Krogh Andersen, E. *Solid State Ionics* **1988**, *26*, 229.
(12) Sudreau, F.; Petit, D.; Boilot, J. P. *J. Solid State Chem.* **1989**, *83*, 78.
(13) Alamo, J.; Rodrigo, J. L. *Solid State Ionics* **1989**, *32/33*, 70.
(14) Perret, R.; Boudjada, A. *C. R. Acad. Sci. Paris* **1976**, *282*, C-245.
(15) Winand, J. M.; Rulmont, A.; Tarte, P. *J. Solid State Chem.* **1991**, *93*, 341.
(16) Martinez, A.; Rojo, J. M.; Iglesias, J. E.; Sanz, J.; Rojas, R. *Chem. Mater.* **1994**, *6*, 1790.
(17) Medeiros, M. E.; Alves, O. L. *Thermochim. Acta* **1994**, *241*, 33.
(18) Shannon, R. D.; Taylor, B. E.; English, A. D.; Berzins, T. *Electrochim. Acta* **1977**, *22*, 783.
(19) Taylor, B. E.; English, A. D.; Berzins, T. *Mater. Res. Bull.* **1977**, *12*, 171.
(20) d'Yvoire, F.; Pintard-Screpel, M.; Bretey, E.; de la Rochere, M. *Solid State Ionics* **1983**, *9/10*, 851.
(21) Subramanian, M. A.; Subramanian, R.; Clearfield, A. *Solid State Ionics* **1986**, *18/19*, 562.
(22) Hamdoune, S.; Tran Qui, D.; Schouler, E. J. L. *Solid State Ionics* **1986**, *18/19*, 587.

0897-4756/95/2807-1857$09.00/0

cal properties. Thus, a change in conductivity and activation energy has been often observed.[1,11,12,28]

The aim of this work is to study the structural modifications of $LiSn_2(PO_4)_3$ when it is heated and cooled in the range 10−250 °C. In particular, the change of symmetry and the enthalpy associated with it have been ascertained by XRD, NMR (^{119}Sn, ^{31}P, and ^{7}Li), and DSC techniques. The ionic conductivity corresponding to each symmetry as well as its variation during the phase transformation have been also determined.

Experimental Section

Phase I of $LiSn_2(PO_4)_3$ was prepared by calcination at 1200 °C of a stoichiometric mixture of Li_2CO_3 (Fluka, >99%), SnO_2 (Aldrich, 99.9%), and $(NH_4)_2HPO_4$ (Fluka, >99%). The reagents were dried at 100 °C for 12 h, and then stoichiometric amounts of these compounds were thoroughly mixed and calcined in a platinum crucible at the following temperatures: 180, 300, 450, 600, 700, 800, 1000, and 1200 °C. Thermal treatments were accumulative up to 1200 °C. The heating and cooling rates between room temperature and those temperatures were 5 °C/min. At each defined temperature the time spent was 6 h in the range 180−700 °C and 24 h above 700 °C. The mixture was ground before and after each thermal treatment.

X-ray powder diffractograms were taken at different temperatures in the range 20−200 °C by using a high-temperature AP HTK 10 camera adapted to a PW 1050/25 Philips diffractometer. The sample was suspended in acetone and transferred as a slurry to a platinum heating plate, where capillarity held the particles after acetone was evaporated. In the heating and cooling experiments the increment of temperature was 10 °C. The sample was subjected at each temperature for 15 min. The patterns were obtained at the indicated temperatures with the exception of that at 10 °C, in which case the pattern was recorded at room temperature although the sample was previously kept at 10 °C for 15 min. The peaks were fitted with $K\alpha_1-K\alpha_2$ doublets, and the position of each peak was taken to be that of the $K\alpha_1$ component, for which a wavelength λ (Cu $K\alpha_1$) = 1.540 5981 Å was assumed.

^{119}Sn, ^{31}P, and ^{7}Li MAS NMR spectra were obtained at different temperatures in the range 20−140 °C by using a B-VT 1000/SU07 unit adapted to an MSL 400 Bruker spectrometer. In the heating and cooling runs the increment of temperature was 10 °C. The sample was previously kept at each temperature for 15 min before the spectra were recorded. The spectrum labeled 10 °C was obtained at room temperature although the sample was subjected at 10 °C for 15 min. Experimental limitations prevented us from obtaining spectra above 140 °C. The frequency used for the ^{119}Sn, ^{31}P, and ^{7}Li spectra was 149.11, 161.96, and 155.50 MHz, respectively. The sample was spun in the range 1.5−3.5 kHz. The spectra were taken after $\pi/2$ pulse irradiation (5 μs for ^{7}Li, and 4 μs for ^{119}Sn and ^{31}P). A time interval between successive scans of 30 s for the three types of spectra was chosen. The number of scans was in the range 1−10. The ^{7}Li and ^{31}P chemical shift values are given relative to 1 M LiCl and 85% H_3PO_4 aqueous solutions, respectively. The reference for the ^{119}Sn spectra was a 5% solution of tetramethyltin in dichloromethane.

A differential scanning calorimeter (Seiko 220 C) was used to determine the enthalpy associated with the structural transformation of $LiSn_2(PO_4)_3$ when it is heated and cooled in the ranges 20 to 250 and 250 to −90 °C. The heating and cooling rates were 5 °C/min. The experiments were carried out under a N_2 flow (50 mL/min).

Electrical conductivity measurements were carried out by the complex impedance method using a 1174 Solartron frequency response analyzer. Autocoherent pellets of phase I could not be used due to their fragility to handling.[15] To overcome this difficulty, a small amount of Teflon (1.2 wt %) was added and mixed with the sample, then pellets of ca. 6 mm diameter and 1 mm thickness were prepared. Teflon was chosen because its electrical conductivity is negligible and that amount was the minimal one to ensure good mechanical properties. Gold electrodes were deposited on the two faces of the pellets by vacuum evaporation. The frequency range used was $10^{-1}-10^{5}$ Hz. The measurements were carried out at different temperatures in the range 60−250 °C with the pellet under a nitrogen flow. In the heating and cooling runs the increment of temperature was 10 °C, and before each measurement the sample was kept at the indicated temperature for 20 min.

Results

XRD. The X-ray diffraction patterns (2θ = 19−22°) corresponding to phase I of $LiSn_2(PO_4)_3$ heated at increasing temperatures between 20 and 200 °C and then cooled from 200 to 10 °C are shown in Figure 1 (top). At 20 °C two peaks at 4.213 and 4.438 Å are observed. When the sample is heated up to 120 °C the doublet is not appreciably modified but between 120 and 200 °C the doublet disappears from the pattern, and two new peaks at 4.321 and 4.376 Å are progressively developed. At 200 °C only the new internal doublet is observed. After this treatment the sample was cooled. Between 200 and 60 °C the pattern is not appreciably modified, and below 60 °C the external doublet grows at the expense of the internal one. At 10 °C only the external doublet, characteristic of phase I, is observed.

The X-ray diffraction patterns recorded at 20 and 200 °C in the range 2θ = 5−60° are shown in Figure 1 (bottom). The pattern at 20 °C, corresponding to phase I, has been previously indexed[16] while the pattern at 200 °C has been indexed in this work.

^{119}Sn, ^{31}P, and ^{7}Li MAS NMR. The NMR spectra of phase I heated in the range 20−140 °C and then cooled from 140 to 10 °C are shown in Figure 2. The ^{119}Sn spectrum at 20 °C consists of two lines at −816 and −833 ppm, and sidebands associated with those lines. The intensity of each line is affected by the contribution of a sideband belonging to the other line. When each line plus its associated sidebands are considered, a 1:1 intensity ratio is obtained. At increas-

(23) Lin, Z.; Yu, H.; Li, S.; Tian, S. *Solid State Ionics* **1986**, *18/19*, 549.
(24) Delmas, C.; Nadiri, A.; Soubeyroux, J. L. *Solid State Ionics* **1988**, *28−30*, 419.
(25) Chowdari, B. V. R.; Radhakrishnan, K. A.; Thomas, K. A.; Subba Rao, G. V. *Mater. Res. Bull.* **1989**, *24*, 221.
(26) Winand, J. M.; Depireux, J. *Europhys. Lett.* **1989**, *8*, 447.
(27) Aono, H.; Sugimoto, E.; Sadaoka, Y.; Imanaka, N.; Adachi, G. *J. Electrochem. Soc.* **1990**, *137*, 1023.
(28) Pronin, I. S.; Sigaryov, S. E.; Vashman, A. A. *Solid State Ionics* **1990**, *38*, 9.
(29) Tillement, O.; Couturier, J. C.; Angenault, J.; Quarton, M. *Solid State Ionics* **1991**, *48*, 249.
(30) Wang, S.; Hwu, S.-J. *J. Solid State Chem.* **1991**, *90*, 377.
(31) Ado, K.; Saito, Y.; Asai, T.; Hiroyuki, K.; Nakamura, O. *Solid State Ionics* **1992**, *53−56*, 723.
(32) Nomura, K.; Ikeda, S.; Ito, K.; Einaga, H. *Solid State Ionics* **1993**, *61*, 293.
(33) Winand, J. M.; Rulmont, A.; Tarte, P. *J. Solid State Chem.* **1993**, *107*, 356.
(34) Amatucci, G. G.; Safari, A.; Shokoohi, F. K.; Wilkens, B. J. *Solid State Ionics* **1993**, *60*, 357.
(35) Aono, H.; Sugimoto, E.; Sadaoka, Y.; Imanaka, N.; Adachi, G. *J. Electrochem. Soc.* **1993**, *140*, 1827.
(36) Warner, T. E.; Milius, W.; Maier, J. *Solid State Ionics* **1994**, *74*, 119.
(37) Zhao, W.; Chen, L.; Xue, R.; Min, J.; Cui, W. *Solid State Ionics* **1994**, *70/71*, 144.
(38) Ikeda, S.; Nomura, K.; Ito, K.; Einaga, H. *Solid State Ionics* **1994**, *70/71*, 153.
(39) Kuwano, J.; Sato, N.; Kato, M.; Takano, K. *Solid State Ionics* **1994**, *70/71*, 332.

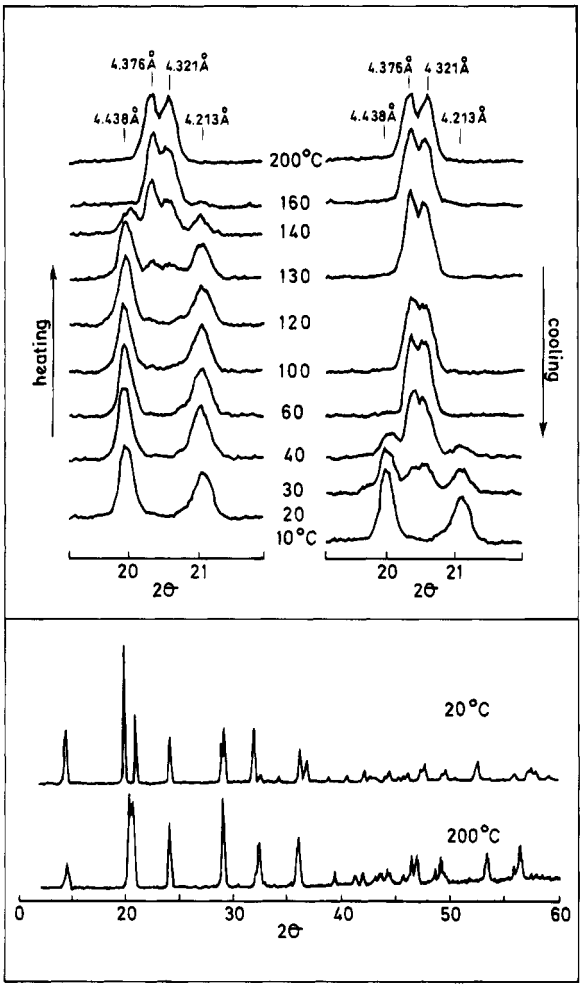

Figure 1. Top: X-ray diffraction patterns (2θ = 19–22°) recorded at the indicated temperatures. Phase I was heated between 20 and 200 °C, and then cooled from 200 to 10 °C. Bottom: X-ray diffraction patterns recorded at 20 and 200 °C in the range 2θ = 5–60°.

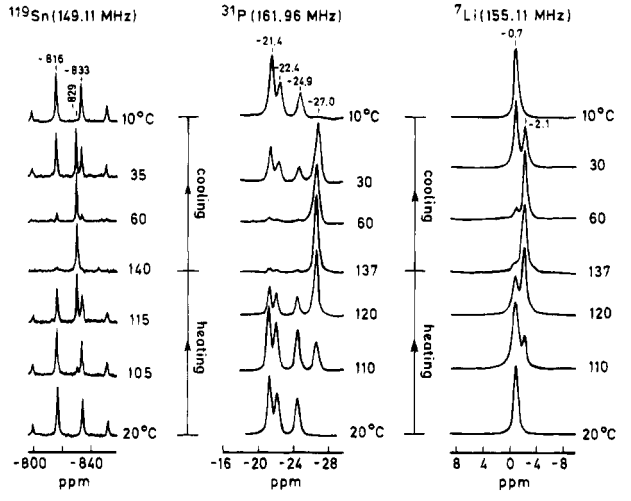

Figure 2. ^{119}Sn, ^{31}P, and ^{7}Li MAS NMR spectra recorded at the indicated temperatures. Phase I was heated between 20 and 200 °C, and then cooled from 200 to 10 °C.

ing temperatures between 20 and 100 °C the spectrum is not appreciably modified. Above 100 °C a new line at −829 ppm is observed; this line grows at the expense of the two former ones with temperature, and at 140 °C the spectrum is mostly formed by the new line. After the heating treatment, the sample was progressively

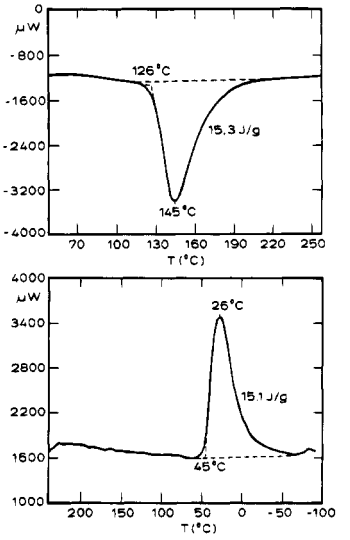

Figure 3. DSC curves corresponding to the heating and cooling treatments of $LiSn_2(PO_4)_3$. The starting phase I was heated in the range 20–250 °C (top) and then cooled to between 250 and −90 °C (bottom).

cooled. Between 140 and 60 °C the spectrum is not appreciably modified showing the line at −829 ppm. At 60 °C the two lines at −816 and −833 ppm are again observed, and they grow at the expense of the −829 ppm line between 60 and 10 °C. At 10 °C the spectrum shows only the starting lines at −816 and −833 ppm.

The ^{31}P spectrum recorded at 20 °C is formed by three lines at −21.4, −22.4, and −24.9 ppm. From the intensity of these lines and their associated sidebands, a 1:1:1 ratio has been deduced. When phase I is heated to between 20 and 100 °C, the spectrum is not appreciably modified. At 100 °C a new line at −27.0 ppm is observed, and above 100 °C the −27.0 ppm line grows as the three former lines diminish. At 140 °C the spectrum is mostly formed by the new line. After this treatment the sample was progressively cooled. Between 60 and 10 °C, the intensity of the −27.0 ppm line decreases while an increase in intensity of the −21.4, −22.4, and −24.9 ppm lines is observed. At 10 °C the spectrum coincides with the one started with.

The ^{7}Li spectrum recorded at 20 °C shows a line at −0.7 ppm. This spectrum does not change between 20 and 100 °C, but between 100 and 140 °C a new line at −2.1 ppm, which grows at the expense of the former one, is observed. At 140 °C the spectrum is mostly formed by the new line. After this treatment the sample was cooled in the range 140–10 °C. No modifications in the spectrum are observed between 140 and 60 °C, and below 60 °C the line at −2.1 ppm diminishes while that at −0.7 ppm grows. At 10 °C the spectrum only shows the initial −0.7 ppm line.

DSC. The calorimetric curves obtained by heating phase I in the range 25–250 °C, and then by cooling the sample from 250 to −100 °C are shown in Figure 3. In the heating treatment (top) an endothermic peak whose temperature at the onset and minimum is 126 and 145 °C, respectively, is clearly observed. From the peak area an enthalpy of 15.3 J/g (8.09 kJ/mol) is deduced. In the cooling treatment (bottom) an exothermic peak appears. The temperature corresponding to the onset and maximum of the peak is 45 and 26 °C, respectively. An enthalpy of 15.1 J/g (7.99 kJ/mol) is deduced.

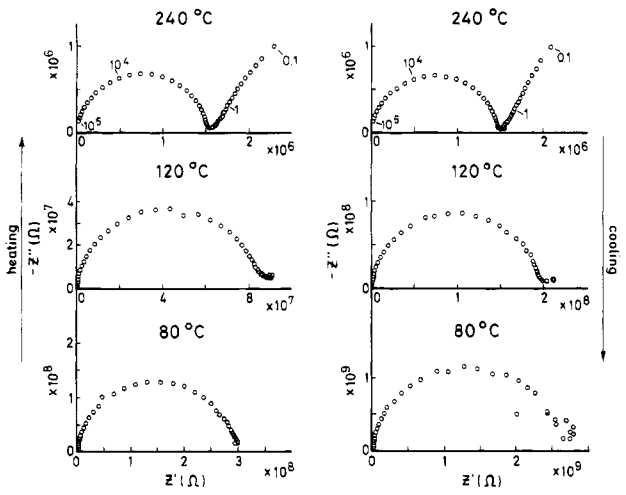

Figure 4. Impedance plots (imaginary vs real part) obtained at the indicated temperatures. Phase I was heated in the range 60–250 °C and then cooled from 250 to 60 °C. Selected frequencies (in hertz) are marked in the plots at 240 °C.

Electrical Measurements. The impedance plots (imaginary $-Z''$ vs real Z') obtained at the indicated temperatures in the heating and cooling treatments are shown in Figure 4. An arc is observed. In addition, at the high temperatures an almost linear spur, which is normally related to blocked charge at the electrode surface, is also detected. The resistance values are derived by extrapolation to the real axis of the low-frequency region of the arcs.

Discussion

Phase I of $LiSn_2(PO_4)_3$ shows a monoclinic *Cc* symmetry as deduced from the NMR and XRD data.[16] In particular, the ^{119}Sn and ^{31}P MAS NMR spectra (Figure 2) consist of two and three equal lines, respectively, indicating the presence of two crystallographic sites for tin and three for phosphorus. The ^{7}Li MAS NMR spectrum shows a line at −0.7 ppm that has been ascribed[16] to Li^+ ions placed in M2 sites. The X-ray diffraction pattern of phase I (pattern recorded at 20 °C in Figure 1) was indexed in a previous work[16] by using a monoclinic cell of parameters $a = 14.665$, $b = 8.405$, $c = 8.893$ Å, $\beta = 122.98°$.

When phase I is heated above 100 °C, it is transformed into another phase. Thus, the ^{119}Sn, ^{31}P, and ^{7}Li lines at −816 and −833 ppm, −21.4, −22.4, and −24.9 ppm, and −0.7 ppm, respectively, which are characteristic of phase I, are progressively removed, and new lines at −829, −27.0, and −2.1 ppm grow at the expense of the first ones. In addition, the X-ray doublet of phase I at 4.438 and 4.213 Å disappears from the patterns, and a new internal doublet at 4.376 and 4.321 Å is observed. The frequency of the new spectral lines and the position of the internal diffraction doublet coincide with the values found for phase II, which was obtained during the formation process.[16] Therefore phase I is transformed into phase II above 100 °C, and at about 160 °C the transformation has finished.

The X-ray diffraction pattern of phase II (see the pattern recorded at 200 °C in Figure 1) has been indexed (Table 1) by using a rhombohedral lattice described by the hexagonal axes: $a_H = 8.642$, $c_H = 21.574$ Å. The usual NASICON $R\bar{3}c$ symmetry is supported for phase II by XRD and NMR data. Thus, the ^{119}Sn, and ^{31}P spectra show one line in both cases (Figure 2), indicating the existence of only one site for tin and another one for phosphorus. The ^{7}Li spectrum shows a line at −2.1 ppm whose frequency is different from that found for phase I. This line has been assigned[16] to Li^+ ions placed in the M1 site, which is the position often reported for NASICON materials with $R\bar{3}c$ symmetry.[1-10] From these results it is clear that the transition from phase I to phase II produces a change of symmetry in the structure from monoclinic to rhombohedral.

Table 1. XRD Powder Pattern of Phase II Recorded at 200 °C

h	*k*	*l*	$2\theta_{calc}$	$2\theta_{obs}$	d_{calc}	d_{obs}	*I*
0	1	2	14.39	14.44	6.149	6.127	5
1	0	4	20.28	20.33	4.376	4.370	100
1	1	0	20.54	20.60	4.321	4.320	90
1	1	3	24.01	24.04	3.704	3.699	64
0	2	4	29.02	29.05	3.075	3.071	80
2	1	1	31.88	31.89	2.805	2.804	16
1	1	6	32.37	32.40	2.764	2.761	85
1	2	2	32.70	32.71	2.736	2.735	8
0	1	8	35.35	35.31	2.537	2.540	7
2	1	4	35.82	35.82	2.505	2.505	71
3	0	0	35.97	35.98	2.495	2.494	56
2	0	8	41.23	41.24	2.188	2.187	12
2	2	0	41.78	41.79	2.1605	2.1600	7
1	1	9	43.12	43.17	2.0962	2.0935	5
1	0	10	43.63	43.63	2.0730	2.0728	28
0	3	6	44.15	44.17	2.0497	2.0489	16
3	1	2	44.41	44.44	2.0384	2.0369	9
1	2	8	46.49	46.49	1.9519	1.9519	56
1	3	4	46.86	46.84	1.9372	1.9379	54
0	2	10	48.68	48.66	1.8691	1.8699	32
2	2	6	49.16	49.17	1.8519	1.8516	48
4	0	4	51.66	51.61	1.7677	1.7694	10
2	1	10	53.36	53.32	1.7155	1.7169	40
1	1	12	55.30	55.29	1.6599	1.6602	5
3	2	4	56.17	56.12	1.6361	1.6376	40
4	1	0	56.28	56.27	1.6332	1.6336	35

To study the reversibility of the transformation, phase II was cooled in the range 140–10 °C. Between 140 and 60 °C the XRD patterns and the NMR spectra are not modified (Figures 1 and 2). However below 60 °C the NMR lines and the external X-ray doublet ascribed to phase I grow at the expense of those corresponding to phase II. At 10 °C only the spectroscopic and diffraction features of phase I are observed. Therefore, phase II is transformed into phase I in a reversible way.

The proportion of transformed phase with temperature has been determined from the intensity of the NMR lines associated with the two phases. These lines, the principal ones and the sidebands, are well fitted by using Lorentzian functions. The percentage of phase II vs sample temperature is plotted in Figure 5. In the heating treatment only above 100 °C a significant increase of phase II is observed, the extent of phase II being close to 90% at 140 °C. In the cooling treatment, between 140 and 60 °C, the relative proportion of both phases does not change; however, below 60 °C a significant decrease of phase II happens, and at 10 °C phase I is completely recovered. Then, a hysteresis cycle in temperature associated with the phase transformation is observed.

Although the detailed crystal structures of the two phases are not available yet, an estimation of the structural change can be made from a comparison of the cell parameters of both phases. For that, monoclinic axes of phase II have been calculated from the hexagonal ones, and they are outlined together with the

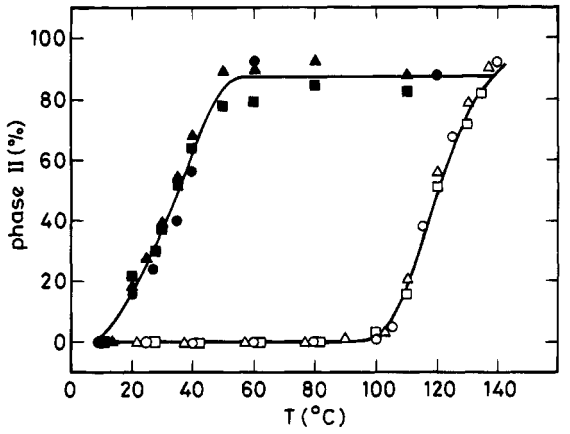

Figure 5. Effect of temperature on the relative proportion of phase II. The values deduced from the intensity of the ^{119}Sn, ^{31}P, and ^{7}Li lines are represented by circles, squares, and triangles, respectively. Open and closed symbols correspond to the heating and cooling treatments, respectively.

Table 2. Cell Parameters of Phases I and II[a] (The Variation of the Parameters for the Phase I to Phase II Transformation Is Also Included)

parameters	phase I	phase II	rel variation (%)
a (Å)	14.666	14.968	2.06
b (Å)	8.405	8.642	2.82
c (Å)	8.893	8.753	−1.57
β (deg)	122.986	124.754	1.44
V (Å^3)	919.51	930.25	1.17

[a] In both cases monoclinic axes are used. For the rhombohedral phase the monoclinic lattice parameters have been derived from the hexagonal parameters (obverse rhombohedron) through the transformation matrix ($1\bar{1}0/110/\bar{1}/3\ 1/3\ 1/3$).

monoclinic axes of phase I in Table 2. A slight variation of the cell parameters in the phase I to phase II transformation can be observed: a, b, and β increase while c decreases. The fact that some parameters increase while others decrease agrees with a modification of the structure more complex than that expected for a pure dilatation. The cell volume becomes greater indicating a first-order transition. The discontinuity observed in the DSC curves supports also the first-order character. The monoclinic-to-rhombohedral transition is endothermic, the reaction going back is exothermic, and in both cases the enthalpy involved is ca. 8 kJ/mol. The coexistence of the two phases in the temperature ranges 100−140 and 60−10 °C points to a transition progressing through nucleation and growth.

From the results reported in this paper it is clear that phase I is stable at low temperatures (about room temperature), while phase II is stable only at higher temperatures (>160 °C). In a previous work[16] we have found that both phases coexist at room temperature in some intermediate stages during the formation of $LiSn_2(PO_4)_3$. This apparent contradiction would be due to an incomplete relaxation of phase II into phase I. To study this point, we have estimated the relative proportion of the two phases in two samples stored at room temperature for ~1.5 years, and we have compared these values with those found during the formation process. One sample is the stoichiometric mixture of Li_2CO_3, $(NH_4)_2HPO_4$, and SnO_2 which was calcined at 550 °C, and the other the same mixture calcined at 700 °C. In the two samples the phase II/phase I ratio was approximately 0.5/0.5,[16] but the amount of other products (SnO_2, SnP_2O_7, and amorphous Li compounds) accompanying phases I and II were clearly different: about 45% and 15% for the samples calcined at 550 and 700 °C, respectively. After the storage at room temperature the unreacted products have remained in the same proportion, but the phase II/phase I ratios have changed. The new values are 0.3/0.7 for the sample calcined at 550 °C and 0.1/0.9 for the sample treated at 700 °C; these values are not appreciably modified by keeping the samples at 10 °C, even at lower temperatures. Then, a portion of phase II has relaxed to phase I in the two cases and is higher when the amount of unreacted products is lower. The last feature suggests that the stabilization of phase II at room temperature is favored by the presence of the unreacted products.

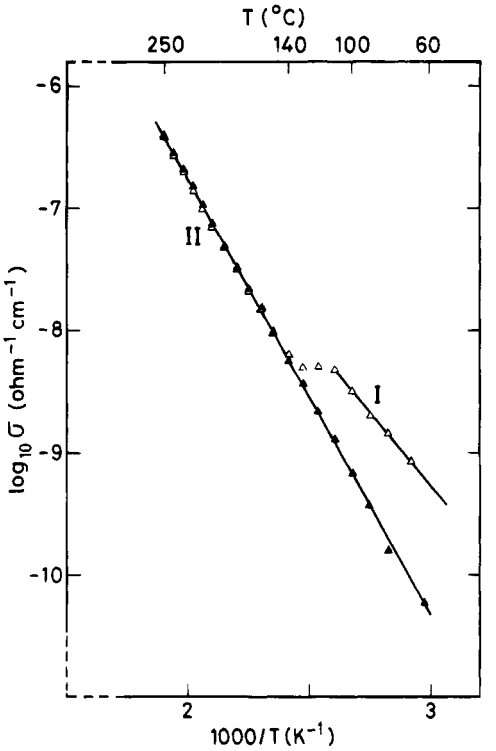

Figure 6. Plot of log σ vs $1000/T$. The starting phase I was heated in the range 60−250 °C (open triangles) and then cooled from 250 to 60 °C (closed triangles). The experimental points are well fitted by two Arrhenius dependences, which are associated with phases I and II.

On the other hand, NASICON materials are, in general, good conductors of alkali ions.[4,19−39] Moreover, $LiSn_2(PO_4)_3$ shows a phase transition that could affect the conductivity associated with diffusion of Li^+ ions. Taking into account that the pellets were prepared by adding a small amount of Teflon, the conductivity values can be considered only relative. Nevertheless, differences in conductivity and activation energy for the two phases have been found.

The variation of conductivity (log σ) vs inverse temperature ($1000/T$) is shown in Figure 6. The values corresponding to the heating and cooling treatments are represented by open and closed triangles, respectively. The experimental points are well fitted by an Arrhenius equation, $\sigma = \sigma_0 \exp(-E/K_BT)$, where σ_0 is a preexponential factor, E the activation energy, and K_B the Boltzman constant. In that figure two linear dependences are observed. According to the XRD and NMR data the straight line found in the heating treatment between 60 and 100 °C is ascribed to phase I. The slight

variation of σ occurring between 100 and 150 °C is related to the monoclinic → rhombohedral transformation. Above 150 °C another linear dependence associated with phase II is observed. In the cooling treatment between 250 and 60 °C, σ follows the last dependence in agreement with stabilization of phase II up to 60 °C, and below 60 °C a change of σ going to the typical dependence of phase I is expected. However, experimental limitations prevented us from measuring of such low σ values. In any case, when the sample was cooled to 10 °C, and impedance measurements were carried out in a second heating–cooling run, the σ values coincided with those obtained in the first cycle, in agreement with the reversible character of the phase transition.

From the slope of the two straight lines, the activation energy (E) associated with motion of Li^+ ions has been determined: values of 0.49 and 0.71 eV are obtained for phases I and II, respectively. Taking into account that in the NASICON structure alkali ions can diffuse within the channels.[1,4,21,40,41] by jumping between the sites M1 and M2, the activation energy deduced from the conductivity data should give a measurement of the energy needed to pass the ions through the bottleneck between the two sites. In our case, the lower E value found in phase I suggests a bigger size of the bottlenecks as compared with phase II.

Conclusions

$LiSn_2(PO_4)_3$ shows a first-order reversible transition accompanied by a hysteresis cycle in temperature. The two phases, I and II, coexist in the temperature ranges 100–160 and 60–10 °C, which points to the transition happening through nucleation and growth.

The symmetry of the low-temperature phase (phase I) is monoclinic Cc, and that of the high-temperature one (phase II) is rhombohedral $R\bar{3}c$. By using a hexagonal cell of parameters $a_H = 8.642$ and $c_H = 21.574$ Å the X-ray diffraction pattern of phase II has been indexed.

The ionic conductivity is higher in phase I as compared to phase II. The activation energies are 0.49 and 0.71 eV for the phases I and II, respectively. A change in conductivity during the phase transition has been also observed.

Acknowledgment. Financial support by CICYT of Spain (Projects MAT 92-0202 and MAT95-0899) is gratefully acknowledged. We thank Dr. Juan P. Belzunegui for calorimetric measurements.

CM950104M

(40) Kohler, H.; Schulz, H.; Melnikov, O. *Mater. Res. Bull.* **1983**, *18*, 1143.
(41) Kohler, H.; Schulz, H. *Mater. Res. Bull.* **1985**, *20*, 1461.